Applied Surface Science 283 (2013) 986–992

Contents lists available at ScienceDirect

Applied Surface Science

journal homepage: www.elsevier.com/locate/apsusc

Use of anionic surfactants for selective polishing of silicon dioxide over silicon nitride films using colloidal silica-based slurries

Naresh K. Penta[1], H.P. Amanapu, B.C. Peethala[2], S.V. Babu*

Department of Chemical and Bimolecular Engineering and Center for Advanced Materials Processing, Clarkson University, Potsdam, NY 13699, USA

ARTICLE INFO

Article history:
Received 2 May 2013
Received in revised form 25 June 2013
Accepted 12 July 2013
Available online 20 July 2013

Keywords:
Anionic surfactants
Zeta potential
Adsorption
Electrostatic interaction
SiO_2
Si_3N_4
CMP
Polish rates

ABSTRACT

Four different anionic surfactants, *sodium dodecyl sulfate*, *dodecyl benzene sulfonic acid* (*DBSA*), *dodecyl phosphate* and *Sodium lauroyl sarcosine*, selected from the sulfate, phosphate, and carboxylic family, were investigated as additives in silica dispersions for selective polishing of silicon dioxide over silicon nitride films. We found that all these anionic surfactants suppress the nitride removal rates (RR) for pH ≤4 while more or less maintaining the oxide RRs, resulting in high oxide-to-nitride RR selectivity. The RR data obtained as a function of pH were explained based on pH dependent distributions of surfactant species, change in the zeta potentials of oxide and nitride surfaces, and thermogravimetric data. It appears that the negatively charged surfactant species preferentially adsorb on the positively charged nitride surface below IEP through its electrostatic interactions and form a bilayer adsorption, resulting in the suppression of nitride RRs. In contrast to the surfactants, K_2SO_4 interacts only weakly with the nitride surface and hence cannot suppress its RR.

1. Introduction

Shallow trench isolation (STI) structures were introduced at the 250 nm technology node to replace traditional LOCOS (local oxidation of silicon) structures and provide better device isolation [1]. The first step in the development of these STI structures involves the deposition of a thin pad oxide as a stress reducer followed by a nitride layer as a hard mask for etching. After patterning the silicon along with the pad oxide and nitride layers, the trenches will be filled with silicon dioxide. Due to inability to deposit selectively, the oxide is deposited over the entire substrate surface. As a result, the oxide deposited over the nitride surface creates an uneven topography that is several hundred nanometers thick. So far chemical mechanical polishing (CMP) has been the only viable technique that can planarize these topographies and achieve local and global planarization. This STI CMP step requires a slurry which polishes the overburden oxide with high oxide removal rate (RR) and stops on the underlying nitride surface, ideally, with no nitride loss.

Ceria abrasives, even without any additives, are known to produce high oxide RRs (>600 nm/min) but also relatively high nitride RRs (>100 nm/min), leading to low RR selectivity (oxide:nitride) [2]. However, ceria-based slurries with various additives [2–8] have seen in widespread use for STI CMP due to their high selectivity of oxide RRs over nitride. Nevertheless, device manufacturers would like to replace these ceria-based slurries due to their tendency to produce a multitude of defects, and more recently, escalating cost, and even uncertainty over availability. These slurries also suffer from low suspension stability. Hence, silica-based slurries have been under investigation as alternatives. Even though silica slurries produce lower oxide RRs compared to ceria and, hence, lower oxide-to-nitride RR selectivity, they have several advantages such as low cost, controllable surface morphology, wide pH range stability and considerably fewer defects. A limited number of additives for silica-based slurries have been investigated to achieve the desirable high RR selectivity with minimal nitride loss [9–12]. Among them, surfactants, especially those selected from the family of sulfonic acid salts, appear to be capable of producing high oxide to nitride RR selectivity [11].

In this work, we show that, besides the sulfonic acid-based surfactants *sodium dodecyl sulfate* (*SDS*) and *dodecyl benzene sulfonic acid* (*DBSA*), phosphate- and carboxylic acid-based surfactants, namely, *dodecyl phosphate* (*DP*) and *sodium lauroyl sarcosine* (*SLS*), respectively, when used as additives in silica slurries, can also suppress the nitride RRs while maintaining the oxide RRs. Furthermore, using the speciation diagrams of these additives, we show that their effects on the RRs of oxide and nitride films are related to the surface charges of SiO_2 and Si_3N_4 determined using zeta potential data. Also, thermo gravimetric measurements were

* Corresponding author.
E-mail address: babu@clarkson.edu (S.V. Babu).
[1] Present address: Dow Electronic Materials, DE, USA.
[2] Present address: IBM, Albany, NY, USA.

0169-4332/$ – see front matter © 2013 Elsevier B.V. All rights reserved.
http://dx.doi.org/10.1016/j.apsusc.2013.07.057

carried out to quantify the additive adsorption at different pH values. It appears that the surfactants preferentially adsorb onto the nitride surfaces through attractive ionic interactions between the negatively charged surfactants and the positively charged nitride surface and hinder direct contact between the nitride surface and silica abrasives, resulting in the suppression of the nitride RRs. Finally, a strategy for post-CMP cleaning of the surfactant is also described.

2. Materials

Colloidal silica ($d_{mean} \sim 50$ nm, BET surface area $\sim 55\ m^2/g$) dispersion used for polishing was supplied by Nyacol Nano Technology. Silicon nitride particles ($d_{mean} \leq \sim 50$ nm, BET surface area $\sim 103\ m^2/g$) used for the zeta potential measurements and thermogravimetric analysis (TGA) were supplied by Sigma–Aldrich. Dodecyl phosphate was obtained from Spectrum Chemicals and the other three surfactants as well as potassium sulfate and pH adjusting agents (KOH and HNO_3) were all obtained from Sigma–Aldrich. All the chemicals except DP are soluble in deionized water, while DP can be easily dissolved in water at pH 11. Hence, to prepare the slurry with DP, it was first dissolved in water at pH 11, followed by addition of silica particles and then adjusting the pH to the desired value. The polishing pad (IC1000) and 4 in. diamond-grit conditioner were supplied by Dow Electronic Materials and 3 M, respectively. Thermal oxide (2000 nm thick, grown at ~900 °C) and silicon nitride (500 nm thick, low pressure chemical vapor deposited at ~790 °C) films, both grown on 8 in. silicon substrates were obtained from Montco-Silicon Technologies Inc. The silicon nitride films have an intervening 100 nm thick silicon dioxide layer between the nitride film and the silicon substrate.

3. Experimental methods

The 8 in. diameter wafers were polished for 1 min on a G&P polisher at 4/5.5 psi wafer/retainer ring pressures, 75/75 rpm carrier/platen speeds, and a slurry flow rate of 200 mL/min. In situ conditioning was performed using a 4 in. diamond grit conditioner. A Filmetrics interferometer was used to measure the thickness of both the films (silicon dioxide and silicon nitride) before and after polishing. The RRs of each of these films were determined from the difference between pre- and post-polished film thickness values. The reported RR for each experiment is the arithmetic average of the RRs measured for two different wafers, each at 20 locations across a diameter of the wafer. The standard deviation in the RRs was calculated based on the data for these 40 locations.

3.1. Thermogravimetric analysis (TGA)

A Perkin-Elmer Thermogravimetric analyzer, Pyris 1, was used to quantify the adsorption of the additive on silica particles (that mimic silicon dioxide films) and silicon nitride particles (used to mimic silicon nitride films). For this purpose, different dispersions containing silica and silicon nitride particles were prepared by adding them to an aqueous solution of the appropriate additive at known concentrations and adjusting to the desired pH. These dispersions were centrifuged at 2000 rpm, the supernatant was decanted, and the solids were redispersed into DI water adjusted to the same pH. This procedure was repeated twice to ensure that the entire unadsorbed and weakly bound additive was removed. The resulting solids were dried for 48 h in an oven maintained at 80 °C and then used for TGA. TGA measures the weight of the sample as the temperature is increased in an inert nitrogen medium. The temperature of the sample was initially raised from room temperature to 100 °C and maintained there for 10 min to remove any remaining moisture and then increased to 650 °C at a rate of 15 °C/min. The reported weight loss data were adjusted by deducting the weight loss of the blank powders and were normalized using particle surface area.

3.2. ζ potential measurements

A Matec Applied science model 9800 Electro acoustic analyzer was used to measure ζ potentials of 10 wt% silica abrasives and 1 wt% silicon nitride particles dispersed in water in the presence and absence of all the surfactants and potassium sulfate as a function of pH. Nitric acid was used to lower the pH while potassium hydroxide was used to increase the pH of the dispersions.

4. Results and discussion

Fig. 1 shows the speciation diagram of the four surfactants investigated. Of these, SDS and DBSA have pK_a values of 1.5 and 2.5, respectively, and have negatively charged species in the experimental pH range 2–10. The phosphate-based surfactant, DP has two pK_a values 2 and 7, and so also has negatively charged species in the same pH range. The carboxylic-based surfactant, SLS, with a pK_a of 3.6, has negatively charged species above ~pH 2.

To understand better the role of the alkyl chain and the functional group in these surfactants, K_2SO_4, which is negatively charged in the pH range 2–10, was also chosen as an additive for comparison. The pK_a values of K_2SO_4 are −3 and 1.9.

Fig. 2 shows the RRs of oxide films obtained using 10 wt% silica dispersions with and without the additives. In the absence of any additive, the RRs of oxide films decrease from ~70 nm/min at pH 2 to ~20 nm/min at pH 4 and 8, and then increase to about 40 nm/min at pH 10. Similar oxide RRs were reported in our earlier publication [13,14]. The decrease in the oxide RRs from pH 2 to 4 is presumably due to the increase in the electrostatic repulsion between the negatively charged silica abrasives and the oxide surface [15] while the increase in the oxide RRs at higher basic pH values can be attributed to an increase in oxide solubility [16].

Basim et al. [17] showed that silica dispersions containing surfactants are very stable at or above critical micelle concentration (CMC) due to the formation of self-assembled micelle-like surfactant structures. Hence, in our case, the additive concentrations were chosen to be close to the CMCs of SDS and DBSA which are ~0.25 wt% and ~0.15 wt%, respectively [12,18]. Since the CMCs of DP and SLS are unknown, 0.15 wt% concentration was also chosen for them. Addition of the three surfactants – SDS, SLS, and DP – increased the oxide RRs at both pH 3 and 4 but not at other pH values, presumably due to the presence of counter ions (K^+ or Na^+), while DBSA caused a smaller increase. Adding 0.25 wt% K_2SO_4, the oxide RRs increased throughout the pH range, presumably due to the increase in ionic strength. Several studies [19–23] have already shown that increasing the ionic strength increases oxide RRs due to the reduction in the electrostatic repulsion, an argument also supported by the ζ potential data for the silica dispersions (later shown in Fig. 4). In spite of these high RRs with K_2SO_4 as an additive, it is a poor candidate for STI slurries since the nitride RRs are also high, as shown below in Fig. 3.

Fig. 3 shows the nitride RRs obtained using the same dispersions. In the absence of any additive, the nitride RRs drop from ~45 nm/min at pH 2 to ~15 nm/min at pH 4 and thereafter follow a trend that is similar to the RRs of oxide films. Similar nitride RRs were reported earlier using the same silica abrasives [14] and discussed based on the electrostatic interactions between the nitride surface and the abrasives. More interestingly, adding either DBSA or SDS suppressed the nitride RRs to ~1 nm/min at both pH 2 and

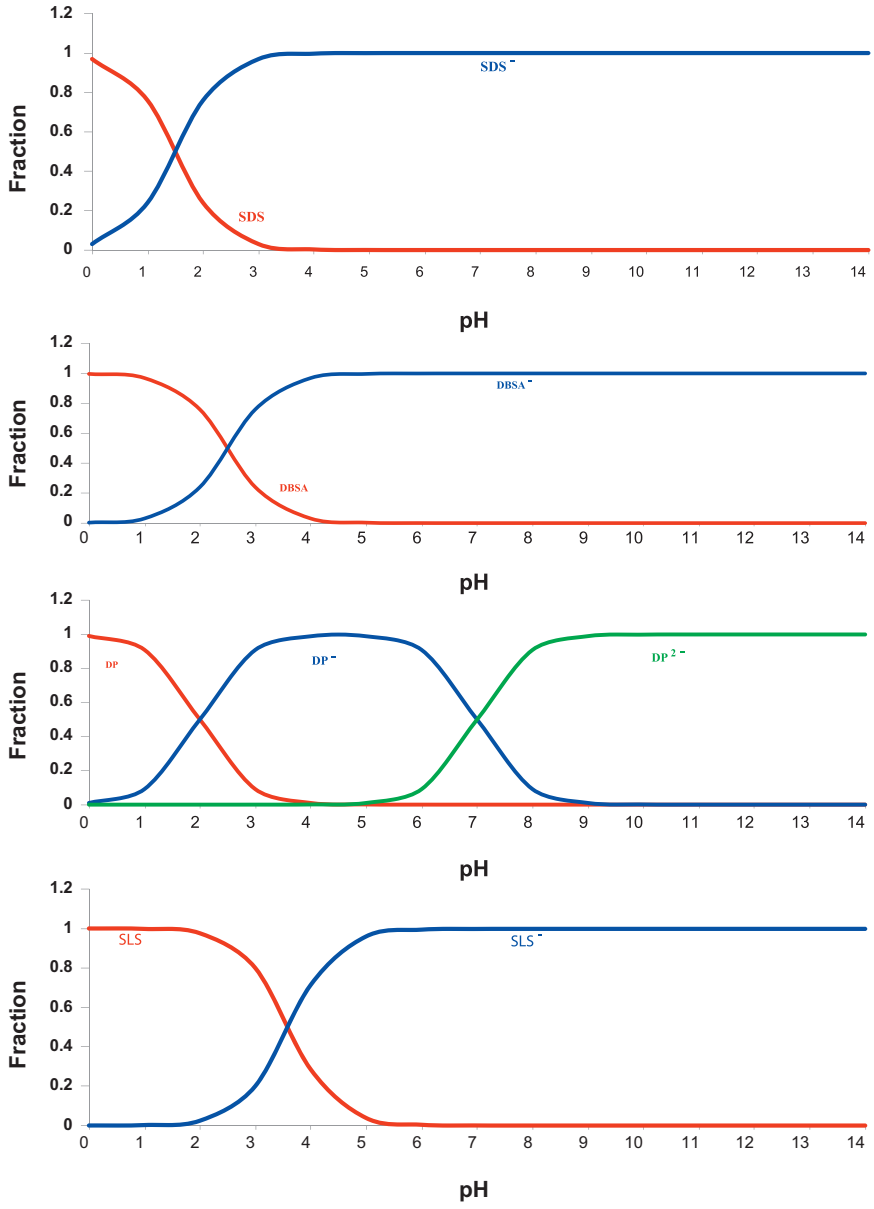

Fig. 1. Speciation diagrams of the four different surfactants: SDS, DBSA, DP and SLS.

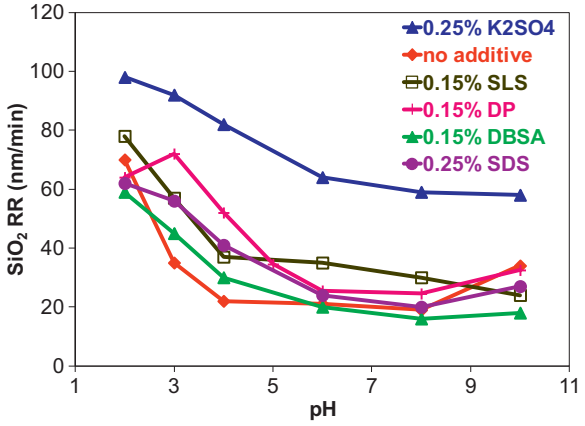

Fig. 2. RRs of oxide obtained using 10 wt% silica ($d_{mean} \sim 50$ nm) dispersions with and without additives.

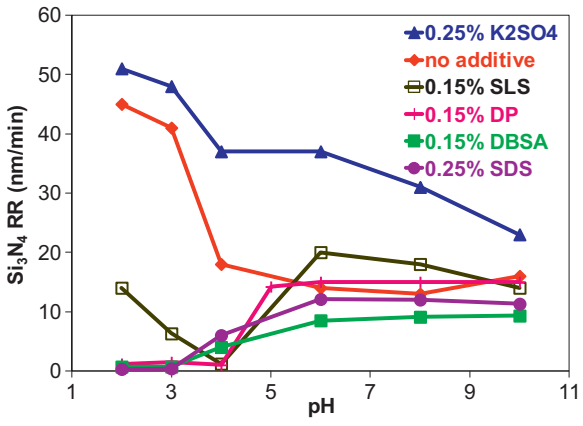

Fig. 3. RRs of nitride obtained using 10 wt% silica ($d_{mean} \sim 50$ nm) dispersions with and without additives.

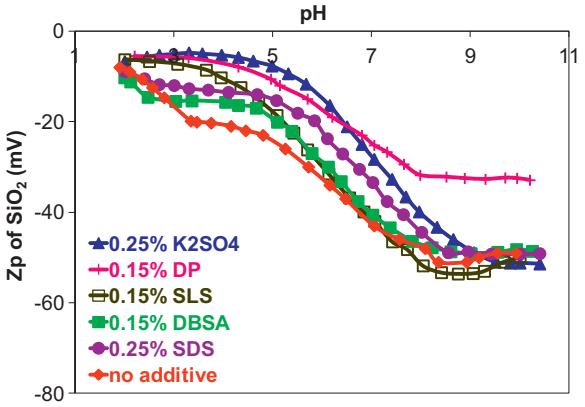

Fig. 4. Zeta potentials (Zp) of 10 wt% silica (d_{mean} ~ 50 nm) dispersions with and without additives.

3 and to ~4 nm/min at pH 4. Beyond pH 5, the RRs remain unaffected. A similar dependence of the nitride RRs obtained using SDS on pH was shown earlier [12]. DP also suppresses the nitride RRs to ~1 nm/min in the pH range 2–4 but does not affect them above pH 4 while SLS suppresses the nitride RR most effectively at pH 4. In sharp contrast, K_2SO_4 enhances the nitride RRs throughout the pH range 2–10.

Before proceeding further, we would like to point out that all four anionic surfactants investigated here suppress the nitride RRs to ~1 nm/min, each in the pH range specified [DBSA (pH 2–3), SDS (pH 2–3), SLS (pH 4) and DP (pH 2–4)], while maintaining the oxide RR, enabling the achievement of the desired selectivity for the STI CMP process.

4.1. ζ potentials of silica surfaces

To understand the mechanism better for the nitride RR suppression with these surfactants, ζ potentials of silica and silicon nitride dispersions were measured as a function pH with and without these additives. The results are shown in Figs. 4 and 5. Fig. 4 shows the ζ potential values of 10% silica dispersions, same particle loading as that used for polishing, with and without the surfactants. In the absence of any additive, silica surface is negatively charged throughout the pH range as is well known. Adding any of the surfactants or K_2SO_4 did not alter the charge much at pH 2 or, with the exception of DP, above pH 9 but increased it more or less for 3 ≤ pH ≤ 9. Addition of DP caused a significant increase in

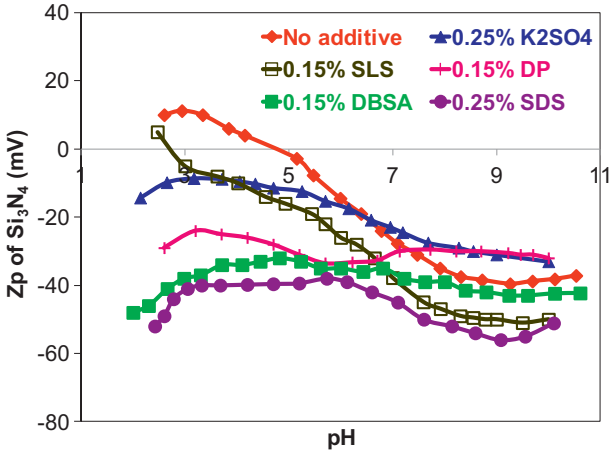

Fig. 5. Zeta potentials (Zp) of 1 wt% silicon nitride particles (d_{mean} ~ 50 nm) dispersions with and without additives.

Table 1
TGA data for particles centrifuged from 1 wt% silica and 1 wt% silicon nitride dispersions containing 0.25 wt% K_2SO_4/0.15 wt% DBSA.

pH	K_2SO_4 remaining ($mg/m^2 \times 10^{-2}$)		DBSA remaining ($mg/m^2 \times 10^{-2}$)	
	Silica	Silicon nitride	Silica	Silicon nitride
2	~1.8	~1	~3	~22
3	<1.8	<1	~1.8	~17
4	<1.8	<1	<1.8	~5
8	<1.8	<1	<1.8	~1

ζ potential above pH 9. All of these solutions have counter ions, either K^+ or Na^+. These ions adsorb on the negatively charged silica surface and increase the ζ potential due to the compression of the surrounding double layer while the negatively charged surfactant molecules/sulfate ions (shown in the speciation diagrams, Fig. 1) are repelled by the negatively charged silica surfaces and do not adsorb. Similar changes in the ζ potential of silica were earlier well documented in the presence of various electrolytes [24–26]. Hence, the change in the ζ potential is attributed mostly to the interaction of counter ions but not to that of the surfactant molecules.

4.2. ζ potentials of silicon nitride surfaces

Fig. 5 shows the ζ potential values of 1 wt% silicon nitride particles dispersed in water with and without adding the surfactants. In the absence of any additives, the IEP of silicon nitride particles is ~5, same as that reported earlier [12,14,27]. The additives reversed the charge of the silicon nitride surface (except for SLS below pH 3) for pH <5 with the ζ potential reaching relatively high negative values, except for SLS and K_2SO_4. For pH ≥5, there is no significant change in the ζ potentials. Hu et al. [28] and Gopal et al. [29] also reported a similar charge reversal of positively charged alumina surfaces in the presence of SDS. Furthermore, the electrokinetic behavior of anatase and several different metal oxides in the presence of sulfate ion containing solutions reported by several authors [30,31] is similar to the data shown in Fig. 5. All of them suggest that sulfate ions diffuse into the electrical double layer surrounding the solid surface and neutralize the positive charge.

From the speciation diagrams (Fig. 1), SDS, DBSA, and DP are mostly negatively charged in the pH range 2–12 while SLS is similarly negatively charged beyond pH 4 while K_2SO_4 will be completely in ionized state. Hence, it appears that the attractive electrostatic interaction between the positively charged nitride surface and the negatively charged additive species drives their adsorption on the nitride surface below its IEP at pH ~5, causing a charge reversal in the zeta potential.

4.3. Differences between the adsorption of K_2SO_4 and DBSA

Even though sulfate ions of both the salt and the surfactants interact with nitride surfaces, only the surfactants suppressed the nitride RRs. To understand this further, thermogravimetric studies were conducted to quantify the amount of the additive adsorption at different pH values. For this experiment, DBSA and K_2SO_4 were chosen as representatives.

Table 1 shows the amounts of adsorbed K_2SO_4 and DBSA remaining on the silica and the silicon nitride surfaces at different pH values after separately centrifuging 1 wt% silica and 1 wt% silicon nitride dispersions containing either 0.25 wt% K_2SO_4 or 0.15 wt% DBSA. There is no significant adsorption of either K_2SO_4 or DBSA on the silica surface, presumably due to the electrostatic repulsion between them and the silica surfaces, as discussed earlier. Also, there is no significant adsorption of K_2SO_4 on the silicon

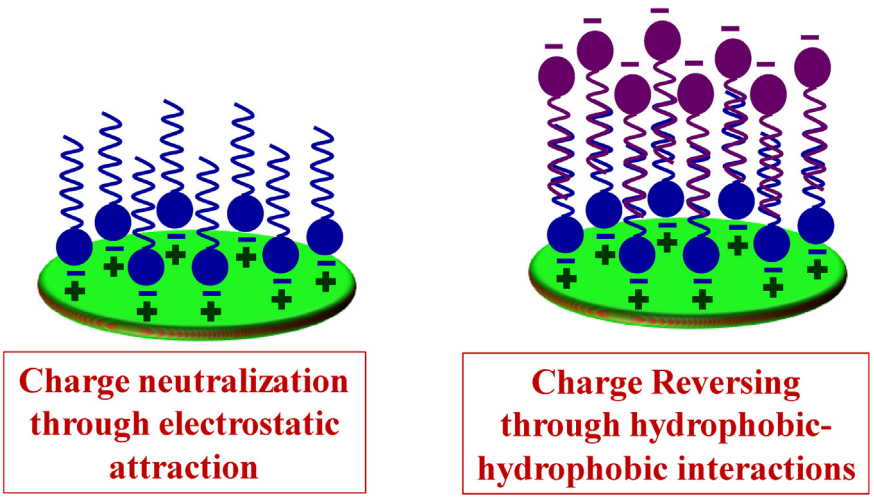

Fig. 6. Schematic of the proposed DBSA adsorption on silicon nitride surface below its IEP.

nitride surfaces despite electrostatic interaction between them, consistent with the ζ potential data above. This suggests that K_2SO_4 interacts only weakly with the silicon nitride surface and hence can be easily removed with centrifuging. In contrast, there is a significant amount of DBSA remaining on the silicon nitride surface at both pH 2 and 3, but the amount drops to $<1 \times 10^{-2}$ mg/m^2 beyond pH 4. A similar adsorption of SDS was found on silicon nitride surface by Bu and Moudgil [12]. These data suggest that DBSA, unlike K_2SO_4, strongly binds to the nitride surface by adsorption driven by electrostatic interactions at pH 2 and 3. This is consistent with the earlier observations of Paria and Khilar [32]. They discussed the effect of cohesive chain-chain interactions among adsorbed surfactant species and hydrophobic chain interactions with hydrophobic sites on the solid as well as the hydration of the adsorbate species on the strength of the surfactant adsorption and showed that the adsorption strength increases with increasing alkyl chain length.

To confirm the differences in the strength of the interaction of K_2SO_4 and DBSA with the nitride surface below its IEP, two dispersions, 1 wt% silicon nitride + 0.25 wt% K_2SO_4 and 1 wt% silicon nitride + 0.15 wt% DBSA, were prepared and adjusted to a pH of 2.5. Their ζ potentials were found to be ~−10 mV and ~−41 mV, respectively. These two dispersions were centrifuged at 2000 rpm and the supernatant was removed. Then, the centrifuged particles were again re-dispersed in water adjusted to the same pH 2.5, and re-centrifuged to remove any weakly bound additive molecules. These centrifuged particles were dispersed a second time in DI water adjusted to the same pH 2.5. Their ζ potentials were remeasured and found to be ~+15 mV and ~−5 mV, respectively. Thus, in the case of K_2SO_4, the original ζ potential of the bare silicon nitride particles was recovered, confirming that K_2SO_4 interacts weakly with the silicon nitride surface and all of it desorbs after centrifuging twice. In contrast, in the case of DBSA, only a portion of the adsorbed DBSA was removed during centrifuging, since the silicon nitride particles retain a small negative charge.

4.4. Proposed adsorption mechanism

Several authors [33–41] investigated the adsorption of cetyltrimethyl ammonium bromide (CTAB), a cationic surfactant, on negatively charged silica surfaces using surface force measurements. They showed that at low surfactant concentrations, CTAB adsorbs through attractive electrostatic interactions to form a monolayer. At higher surfactant concentrations, additional CTAB molecules adsorb on the monolayered interface to form *loosely packed* bilayers through a weak interaction between the hydrophobic hydrocarbon tails of CTAB and the surface begins to gain charge. Hu et al. [28] also observed the formation of bilayers on an alumina surface in the presence of SDS and proposed that hydrophobic interactions are responsible for this bilayer formation.A schematic for the adsorption of anionic DBSA on a silicon nitride surface that is consistent with our ζ potential data, TGA results and the above discussion, is shown in Fig. 6. Initially, DBSA molecules adsorb on the positively charged silicon nitride surface through electrostatic interactions to form a monolayer and neutralize the surface charge. Now, the hydrophobic tails of additional DBSA molecules interact weakly with the hydrophobic tails of the adsorbed DBSA molecules to form *loosely packed* bilayers. These weakly bound layers can be easily broken by centrifuging but the adsorbed monolayer remains intact even after centrifuging at 9500 rpm. A similar mechanism holds for the adsorption of SDS, SLS, and DP.

4.5. Effect of the additive adsorption on oxide and nitride RRs

None of the surfactants studied adsorbs on an oxide surface and, hence, does not suppress the oxide RR. In the case of K_2SO_4, however, the counter ions, K^+, interact with silica surfaces, as suggested by the ζ potential data. The adsorbed cations, as suggested by Choi et al. [22], enable more abrasive particles to come into contact with the wafer surface leading to an increase in the oxide RRs. Also, the adsorbed cations interact with the negatively charged Si—O$^-$ on the surface and weaken the underlying Si—O—Si bonds as suggested by Kawano et al. [42–44]. The weakened bonds are more easily ruptured by the abrasives, again enhancing the RRs.

Our ζ potential results showed that DBSA, SDS, SLS and DP adsorb on the nitride surface below its IEP. More importantly, any bilayers formed on it through hydrophobic–hydrophobic interactions can act as lubrication layers between the abrasive and the wafer as well as block direct contact between them, both resulting in lower nitride RRs. Since K_2SO_4 interacts only weakly with the nitride surface, the adsorbed film can be easily removed by the silica abrasives without impacting the nitride RRs. On the other hand, the adsorption of cations might affect the suboxide present on the nitride surface similar to the oxide films discussed above and enhance the RRs in the presence of K_2SO_4.

4.6. Post-CMP cleaning of DBSA

Desorption of DBSA from the nitride surface was studied to ensure that post-CMP cleaning is not a challenge despite the strong

adsorption. Again DBSA was chosen as a representative. For this purpose, 1 wt% silicon nitride + 0.15 wt% DBSA at pH 2.5 was prepared. The ζ potential of this dispersion is $\sim$−41 mV and from the TGA data in Table 1, the amount of DBSA adsorbed by the nitride particles is $\sim 22 \times 10^{-2}$ mg/m^2. This dispersion was centrifuged for three times at 2000 rpm to ensure the weakly adsorbed additive is removed. The newly obtained centrifuged particles were re-dispersed at pH 10, where both DBSA and nitride surface are negatively charged. This dispersion at pH 10 was centrifuged and the resulting centrifuged particles were re-dispersed back into the pH 2.5 water. The ζ potential of these particles was $\sim$+15 mV, same as that of bare silicon nitride particles. TGA of the particles showed that DBSA remaining was $<22 \times 10^{-2}$ mg/m^2, suggesting that almost all the adsorbed DBSA was removed. This result implies that the adsorption of DBSA on the nitride surface is a reversible electrostatic force-driven process and, hence, post-CMP cleaning in an alkaline environment will be effective.

5. Conclusions

Several silica slurries containing sulfate-, phosphate-, and carboxylic-based surfactants were shown to suppress the nitride RR to $\leq$1 nm/min in the pH range of $\sim$2–4 while maintaining the oxide RRs, facilitating relatively high oxide to nitride selectivity. The nitride RRs were suppressed only at pH values below its IEP by the negatively charged surfactant species present in the slurry. ζ potentials and TGA data showed that these negatively charged species adsorb on the silicon nitride surfaces but not on the oxide surfaces. The adsorbed film likely consists of a bilayer, with the formation of the first layer driven by the attractive electrostatic interactions while that of the secondary layer is through hydrophobic–hydrophobic interactions of the surfactant tails. The TGA data suggest that the hydrophobic–hydrophobic interactions are much weaker than the electrostatic interactions. The adsorbed bilayered surfactant film acts as a passivating layer and hinders the contact between the silica abrasives and the nitride surface, resulting in low nitride RRs. In contrast to the sulfate-based surfactants, K_2SO_4 interacts weakly with a nitride surface and hence does not suppress its RRs. However, it increases oxide RRS.

Acknowledgements

The authors acknowledge Intel Corp. for partial funding of this project, Nyacol Nano Technology for supplying silica dispersions, Dow Electronic Materials for providing IC 1000 pads, and 3M Co. for providing diamond conditioners.

References

[1] K. Blumenstock, J. Theisen, P. Pan, J. Dulak, A. Ticknor, T. Sandwick, K. Blumenstock, J. Theisen, P. Pan, J. Dulak, A. Ticknor, T. Sandwick, Shallow trench isolation for ultra-large-scale integrated devices, Journal of Vacuum Science and Technology B 12 (1994) 54–58.
[2] P.R. Dandu Veera, S. Peddeti, S.V. Babu, Selective chemical mechanical polishing of silicon dioxide over silicon nitride for shallow trench isolation using ceria slurries, Journal of the Electrochemical Society 156 (2009) H936–H943.
[3] S.D. Hosali, A.R. Sethuraman, J.-F. Wang, L.M. Cook, Composition and method for polishing a composite of silica and silicon nitride, U.S. Pat. 5,738,800 (1998).
[4] R. Srinivasan, S.V. Babu, W.G. America, Y.-S. Her, Slurry for chemical mechanical polishing silicon dioxide, U.S. Pat. 6,627,107, 6,544,892, 6,468,910, and 6,491,843.
[5] W.R. Morrison, K.P. Hunt, High selectivity oxide to nitride slurry, U.S. Pat. 5,938,505 (1999).
[6] F. Edelbach, E. Oswald, Y.-S. Her, High selectivity CMP slurry, U.S. Pat. 6,616,514 B1 (2003).
[7] W.-Q. Xu, S. Hegde, CMP slurry, U.S. Pat. 0,028,450 A1 (2005).
[8] M. Fukasawa, N. Koyama, Y. Kurata, K. Haga, T. Akutsu, Y. Ootsuki, CMP polishing agent and method for polishing substrates, U.S. Pat. 0,003,925 A1 (2008).
[9] D.F. Canaperi, R. Jagannathan, M. Krishnan, C.O. Morgan, T.M. Wright, Chemical mechanical polishing of multiple material substrates and slurry having improved selectivity, U.S. Pat. 6,114,249 (2000).
[10] G.S. Grover, B.L. Mueller, Composition for oxide CMP, U.S. Pat. 5,759,917 (1998).
[11] I. Belov, L. Puppe, W. Passing, T.J. Hunt, High selective colloidal silica slurry, U.S. Pat. 6,964,600 B2 (2005).
[12] K.-H. Bu, B.M. Moudgil, Selective chemical mechanical polishing using surfactants, Journal of the Electrochemical Society 154 (2007) H631–H635.
[13] P.R. Dandu Veera, A. Natarajan, S. Hedge, S.V. Babu, Selective polishing of polysilicon during fabrication of microelectromechanical systems devices, Journal of the Electrochemical Society 156 (2009) H487–H494.
[14] N.K. Penta, P.R. Dandu Veera, S.V. Babu, Role of poly(diallyldimethylammonium chloride) in selective polishing of polysilicon over silicon dioxide and silicon nitride films, Langmuir 27 (2011) 3502–3510.
[15] W. Choi, S.-M. Lee, R.K. Singh, pH and down load effects on silicon dioxide dielectric CMP, Electrochemical and Solid-State Letters 7 (2004) G141–G144.
[16] J.T. Abiade, S. Yeruva, W. Choi, B.M. Moudgil, D. Kumar, R.K. Singh, A tribochemical study of ceria–silica interactions for CMP, Journal of the Electrochemical Society 153 (2006) G1001–G1004.
[17] G.B. Basim, I.U. Vakarelski, B.M. Moudgil, Role of interaction forces in controlling the stability and polishing performance of CMP slurries, Journal of Colloid and Interface Science 263 (2003) 506–515.
[18] C.V.V.S. Surisetty, P. Goonetilleke, D. Roy, S.V. Babu, Dissolution inhibition in Cu-CMP using dodecyl-benzene-sulfonic acid surfactant with oxalic acid and glycine as complexing agents, Journal of the Electrochemical Society 155 (2008) H971–H980.
[19] Y. Hayashi, M. Sakurai, T. Nakajima, K. Hayashi, S. Sasaki, S. Chikaki, T. Kunio, Ammonium-salt-added silica slurry for the chemical mechanical polishing of the interlayer dielectric film planarization in ULSI's, Japanese Journal of Applied Physics Part 1 34 (1995) 1037–1042.
[20] K. Rajan, R.K. Singh, J. Adler, U. Mahajan, Y. Rabinovich, B.M. Moudgil, Surface interaction forces in chemical–mechanical planarization, Thin Solid Films 529 (1997) 308–309.
[21] U. Mahajan, M. Bielmann, R.K. Singh, Dynamic lateral force measurements during chemical mechanical polishing of silica, Electrochemical and Solid-State Letters 2 (1999) 80–82.
[22] W. Choi, U. Mahajan, S.-M. Lee, J. Abiade, R.K. Singh, Effect of slurry ionic salts at dielectric silica CMP, Journal of the Electrochemical Society 151 (2004) G185–G189.
[23] S. Ramarajan, Y. Li, M. Hariharaputhiran, Y.-S. Her, S.V. Babu, Effect of pH and ionic strength on chemical mechanical polishing of tantalum, Electrochemical and Solid-State Letters 3 (2000) 232–234.
[24] A. Anderson, M. Tomic, M.J. Gieselmann, The critical gelling point in silica gels containing lithium, sodium and potassium, Journal of Colloid and Interface Science 110 (1989) 17–25.
[25] J. Depasse, A. Watillon, The stability of amorphous colloidal silica, Journal of Colloid and Interface Science 33 (1970) 430–438.
[26] M. Kosmulski, Positive electrokinetic charge of silica in the presence of chlorides, Journal of Colloid and Interface Science 208 (1998) 543–545.
[27] Z. Chen, R.K. Singh, Mechanism of particle deposition on silicon surface during dilute HF cleans, Journal of the Electrochemical Society 150 (2003) G667–G672.
[28] Y. Hu, J. Dai, Hydrophobic aggregation of alumina in surfactant solution, Minerals Engineering 16 (2003) 1167–1172.
[29] T. Gopal, J.B. Talbot, Effects of CMP slurry chemistry on the zeta potential of alumina abrasives, Journal of the Electrochemical Society 153 (2006) G622–G625.
[30] M. Kosmulski, J.B. Rosenholm, High ionic strength electrokinetics of anatase in the presence of multivalent inorganic ions, Colloids and Surfaces A: Physicochemical and Engineering Aspects 248 (2004) 121–126.
[31] M. Kosmulski, Chemical Properties of Materials Surfaces, Dekker, 2001.
[32] S. Paria, K.C. Khilar, A review on experimental studies of surfactant adsorption at the hydrophilic solid–water interface, Advances in colloid and interface science 110 (2004) 75–95.
[33] L.M. He, L.W. Zelazny, V.C. Baligar, K.D. Ritchey, D.C. Martens, Ionic strength effects on sulfate and phosphate adsorption on γ-alumina and kaolinite: triple-layer model, Soil Science Society of America Journal 61 (1997) 784–793.
[34] R.M. Pashley, J.N. Israelachvili, A comparison of surface forces and interfacial properties of mica in purified surfactant solutions, Colloids and Surfaces 2 (1981) 169–187.
[35] J.N. Israelachvili, R.M. Pashley, Measurement of the hydrophobic interaction between two hydrophobic surfaces in aqueous electrolyte solutions, Journal of Colloid and Interface Science 98 (1984) 500–514.
[36] R.M. Pashley, B.W. Ninham, Double-layer forces in ionic micellar solutions, Journal of Physical Chemistry 91 (1987) 2902–2904.
[37] R.M. Pashley, P.M. McGuiggan, R.G. Horn, B.W. Ninham, Forces between bilayers of cetyltrimethylammonium bromide in micellar solutions, Journal of Colloid and Interface Science 126 (1988) 569–578.
[38] P. Kekicheff, H.K. Christenson, B.W. Ninham, Adsorption of cetyltrimethylammonium bromide to mica surfaces below the critical micellar concentration, Colloids and Surfaces 40 (1989) 31–41.
[39] J.L. Parker, V.Y. Yaminsky, P.M. Claesson, Surface forces between glass surfaces in cetyltrimethylammonium bromide solutions, Journal of Physical Chemistry 97 (1993) 7706–7710.
[40] R. Podgornik, V.A. Parsegian, Forces between CTAB-covered glass surfaces interpreted as an interaction-driven surface instability, Journal of Physical Chemistry 99 (1995) 9491–9496.

[41] K. Esumi, M. Matoba, Y. Yamanaka, Characterization of adsorption of quaternary ammonium cationic surfactants and their adsolubilization behaviors on silica, Langmuir 12 (1996) 2130–2135.
[42] M. Kawano, S. Obokata, The effect of amino acids on the dissolution rates of amorphous silica in near-neutral solution, Clays and Clay Minerals 55 (2007) 361–368.
[43] M. Kawano, T. Hatta, J. Hwang, Enhancement of dissolution rates of amorphous silica by interaction with amino acids in solution at pH 4, Clays and Clay Minerals 57 (2009) 161–167.
[44] M. Kawano, J. Hwang, Enhancement of dissolution rates of amorphous silica by interaction with bovine serum albumin at different pH conditions, Clays and Clay Minerals 58 (2010) 272–279.